

The Velocity-Dependent J -factor of the Milky Way Halo: Does What Happens in the Galactic Bulge Stay in the Galactic Bulge?

Kenny Kiriu,^a Jason Kumar,^a Jack Runburg^a

^aDepartment of Physics & Astronomy, University of Hawai'i, Honolulu, HI 96822, USA

E-mail: kiriuk@hawaii.edu, jkumar@hawaii.edu, runburg@hawaii.edu

Abstract. We consider the angular distribution of the photon signal which could arise from velocity-dependent dark matter annihilation within the Galactic bulge. We find that, for the case of Sommerfeld-enhanced annihilation, dark matter annihilation within the bulge is dominated by slow speed particles which never leave the bulge, allowing one to find a simple analytic relationship between the dark matter profile within the Galactic bulge and the angular distribution. On the other hand, for the case p - or d -wave annihilation, we find that the small fraction of high-speed particles which can leave the bulge provide a significant, often dominant, contribution to dark matter annihilation within the bulge. For these scenarios, fully understanding dark matter annihilation deep within the Galactic bulge, and the angular distribution of the resulting photon signal, requires an understanding of the dark matter profile well outside the bulge. We consider the Galactic Center excess in light of these results, and find that an explanation of this excess in terms of p -wave annihilation would require the dark matter profile within the bulge to have a much steeper profile than usually considered, but with uncertainties related to the behavior of the profile outside the bulge.

Keywords: dark matter theory, dark matter experiments, Milky Way

Contents

1	Introduction	1
2	Dark matter and baryons near the galactic center	3
3	Analytic Approximation	4
3.1	Validity of the Analytic Approximation	6
4	The Galactic Center Excess	9
5	Conclusion	11

1 Introduction

The Galactic Center (GC) of the Milky Way (MW) is an interesting target for the indirect detection of dark matter, because it is expected to have a large density of dark matter (DM). In fact, an excess of gamma-rays in the GeV range has been observed within the inner several degrees of the GC [1–3]. The origin of these photons is under study, and may lie in ordinary astrophysical sources, such as millisecond pulsars (MSPs) (see, for example, [4]). Dark matter is another possible origin which has been the subject of much study, particularly because the angular distribution seen in the photon excess is consistent with what one would expect from dark matter annihilation, assuming a density distribution consistent with results from numerical simulations. In this work, we will study the dependence of the gamma-ray angular distribution on the velocity-dependence of dark matter annihilation. Although our analysis will be general, we will consider an application of these results to the observed GC excess, assuming its origin is dark matter annihilation.

The velocity-dependence of the dark matter annihilation cross section impacts the consistency of a dark matter explanation for the GC excess with constraints from searches of dwarf spheroidal galaxies (dSphs) [5–9]. In the most commonly studied scenario (s -wave annihilation) σv is independent of the relative velocity v . In this case, models which can explain the GC excess have cross sections which are roughly at the limit of dSphs searches. Although there are systematic uncertainties which make a clear statement difficult, it is fair to say that an explanation of the GC excess through s -wave dark matter annihilation faces non-trivial constraints from dSphs searches [9–11]. But if dark matter annihilates from a p - or d -wave initial state, then annihilation is more heavily suppressed in regions where the dark matter relative velocity is smaller, suppressing the annihilation rate in dSphs relative to the GC. Since these scenarios effectively weaken any constraints from dSphs searches on explanations of the GC excess, it is important to know how these scenarios affect the effective J -factor, which encodes the angular distribution of the signal.

There has already been previous work discussing the effective J -factor of halos in the case of velocity-dependent dark matter annihilation (see, for example, [12–18]), and of the GC in particular [19–22]. The case of the GC is complicated by the fact that there is a large baryonic contribution to the gravitational potential, yielding additional parameters of the baryonic distribution which affect the J -factor. In this work, we will consider dark matter annihilation within the Galactic bulge. Under the approximation that baryonic matter

dominates the gravitational potential, which is taken to have a power-law expansion, one can then solve for the dark matter velocity-distribution and the J -factor analytically in the region of the Galactic bulge.

We will find that for Sommerfeld-enhanced dark matter annihilation, the angular distribution in bulge region is dominated by the annihilation of low-speed particles which never leave the bulge, resulting in a simple analytic prediction for the angular distribution which depends only on the slope of the dark matter profile inside the bulge. This analytic prediction for the angular distribution can be applied to a wide range of scenarios, including different choices for the dark matter density profile outside the Galactic bulge.

On the other hand, we find that the p -wave and d -wave annihilation rates receive a sizeable contribution from the energetic particles which explore the gravitational potential far outside the bulge. Although such particles only provide a negligible contribution to the dark matter density inside the bulge, they are the fastest particles, and thus may dominate the annihilation rate within the bulge. In this case, one cannot disentangle the angular distribution of the signal near the GC from the gravitational potential far from the GC. As a result, one will see deviations from the analytic prediction which depend on the steepness of the dark matter profile, and find that a complete description of the angular distribution at small angle requires knowledge of the dark matter distribution even well outside the bulge.

It is generally difficult to determine the behavior of dark matter within the bulge region. Stellar data can be used to constrain the density distribution within the bulge, but there are large uncertainties associated with the complexity of the stellar populations. Results can also be obtained from numerical simulations, but these simulations often lack the resolution to adequately probe the bulge (for recent progress, see [22]). Standard density profiles, such as NFW (or generalized versions of NFW), typically assume a power-law behavior all the way out to the scale radius ($r_s \sim 21$ kpc), but there is no particular reason why there cannot be a different power-law behavior within the bulge itself, where the baryonic potential is more important. It is thus important to understand the circumstances in which the photon angular distribution depend only on the dark matter profile near the bulge, and how important corrections due to the behavior outside the bulge can be.

It has been found that, for s -wave annihilation, the GC excess morphology can be matched by a dark matter density profile which scales as $\rho(r) \propto r^{-\gamma}$ with γ in the range 1.2–1.4 (see, for example, [2, 23]). For the case of p -wave annihilation, we find that the same morphology may require a steeper profile. Even so, we find that an accurate model of the photon angular distribution within the bulge requires knowledge of particles which exit the bulge. This implies that ambiguities in the dark matter profile and the effects of triaxiality, for example, can have a significant effect on the angular distribution for p -wave annihilation in the GC region.

The plan of this paper is as follows. In Section 2, we describe the general formalism for computing the velocity-dependent J -factor in the Galactic bulge region. In Section 3, we describe an analytic approximation to the angular distribution, and the considerations which affect its validity. In Section 4, we apply these results to the GC excess. We conclude with a discussion of our results in Section 5.

2 Dark matter and baryons near the galactic center

We consider the case in which the dark matter annihilation cross section has a velocity dependence which can be expressed as

$$\sigma v = (\sigma v)_0 \times (v/c)^n, \quad (2.1)$$

where v is the relative speed and $(\sigma v)_0$ is a constant which is independent of v . The most common example is dark matter annihilation from an s -wave initial state ($n = 0$), in which case σv is independent of v in the non-relativistic limit. But there are a variety of well-motivated scenarios which are worth considering. If dark matter annihilates from a p -wave initial state, then one would find $n = 2$; this scenario can arise, for example, if dark matter is a Majorana fermion which couples to a Standard Model (SM) fermions/anti-fermion pair through interactions which respect minimal flavor violation (MFV) (see, for example, [24]). If the dominant annihilation channel is from a d -wave initial state, then one would find $n = 4$; this scenario can arise if dark matter were instead a self-conjugate spin-0 particle [24–26]. If dark matter annihilation is Sommerfeld-enhanced due to an attractive force mediated by a nearly massless particle, one would find $n = -1$ [27, 28].

If we assume that the dark matter is a self-conjugate particle, we can express the photon flux arising from dark matter annihilation in the Milky Way halo as

$$\frac{d^2\Phi}{dEd\Omega} = \frac{(\sigma v)_0}{8\pi m_X^2} \frac{dN}{dE} J_S(\cos\theta), \quad (2.2)$$

where m_X is the dark matter mass, dN/dE is the photon energy spectrum arising from dark matter annihilation, and

$$J_S(\cos\theta) = \int d\ell \int d^3v_1 f(r(\ell, \theta), v_1) \int d^3v_2 f(r(\ell, \theta), v_2) \times (|\vec{v}_1 - \vec{v}_2|/c)^n. \quad (2.3)$$

Here, $f(r, v)$ is the dark matter velocity-distribution within the halo, which we assume is spherically symmetric and isotropic. This essentially implies that f is a function only of $r = |\vec{r}|$ and $v = |\vec{v}|$. D is the distance to the GC, θ is the angle between the GC and the line-of-sight, and $\ell = D \cos\theta \pm \sqrt{|\vec{r}|^2 - D^2 \sin^2\theta}$ is the distance along the line-of-sight.

It will be convenient to express $J_S(\cos\theta)$ as

$$\begin{aligned} J_S(\cos\theta) &= \int_0^\infty d\ell P_n^2(r), \\ &\sim 2 \int_{D \sin\theta}^\infty dr \left(1 - \frac{D^2}{r^2} \sin^2\theta\right)^{-1/2} P_n^2(r), \end{aligned} \quad (2.4)$$

where

$$\begin{aligned} P_n^2(r) &= \int d^3v_1 \int d^3v_2 f(r, v_1) f(r, v_2) \times (|\vec{v}_1 - \vec{v}_2|/c)^n, \\ &= 8\pi^2 \int_0^\infty dv_1 \int_0^\infty dv_2 v_1^2 v_2^2 f(r, v_1) f(r, v_2) \frac{(v_1 + v_2)^{n+2} - |v_1 - v_2|^{n+2}}{(n+2)v_1 v_2 c^n}. \end{aligned} \quad (2.5)$$

Note that the upper limit integration in the second line of eq. 2.4 encompass negative values of ℓ , including integration along the line-of-sight in both directions. But when observing near the GC, the associated error is negligible.

To determine the J -factor, we need an expression for $f(r, v)$. It follows from Liouville's Theorem that the time-averaged velocity-distribution can only be a function of the energy, as this is the only relevant integral of motion for a classical orbit. Defining $f(r, v) = f(E(r, v))$, where $E = (1/2)v^2 + \Phi(r)$ is the energy per mass of a dark matter particle, and $\Phi(r)$ is the gravitational potential, we have

$$\begin{aligned}\rho(r) &= 4\pi \int_0^{v_{esc}(r)} dv v^2 f(r, v), \\ &= 4\sqrt{2}\pi \int_{\Phi(r)}^{\Phi(\infty)} dE \sqrt{E - \Phi(r)} f(E),\end{aligned}\tag{2.6}$$

where $v_{esc}(r)$ is the galactic escape velocity at r . Inverting this equation with the Abel integral equation yields the Eddington inversion formula

$$f(E) = \frac{1}{\sqrt{8}\pi^2} \int_E^{\Phi(\infty)} \frac{d^2\rho}{d\Phi^2} \frac{d\Phi}{\sqrt{\Phi - E}},\tag{2.7}$$

where we have implicitly expressed ρ as a function of Φ . We may write the gravitational potential $\Phi = \Phi_{DM} + \Phi_{bary}$ as the sum of the potential due to dark matter and the potential due to baryonic matter in the Milky Way, with

$$\Phi_{DM}(r) = \Phi_{DM}(0) + 4\pi G_N \int_0^r \frac{dx}{x^2} \int_0^x dy y^2 \rho(y).\tag{2.8}$$

We utilize a spherical approximation to the gravitational potential due to baryonic matter in the bulge and the disk [29, 30], yielding

$$\Phi_{bary}(r) = -G_N \left[\frac{M_b}{c_0 + r} + \frac{M_d}{r} \left(1 - e^{-r/b_d} \right) \right] + G_N \left[\frac{M_b}{c_0} + \frac{M_d}{b_d} \right],\tag{2.9}$$

where we take $M_b = 1.5 \times 10^{10} M_\odot$ as the mass of the Galactic bulge and $M_d = 7 \times 10^{10} M_\odot$ as the mass of the Galactic disk. We take the bulge scale radius to be $c_0 = 0.6$ kpc, and the disk scale radius to be $b_d = 4$ kpc. We have added a convenient constant to the potential to set $\Phi(0) = 0$. Note, we are ignoring the contribution to the gravitational potential due to the black hole at the center of the Milky Way. This contribution should be subleading for $r > \text{pc}$ (see [31], for example).

Given an ansatz for $\rho(r)$, one can then numerically integrate the above equations to obtain $J_S(\cos\theta)$ [19]. We will consider generalized NFW profiles, given by

$$\rho(r) = \frac{\rho_s}{(r/r_s)^\gamma (1 + (r/r_s))^{3-\gamma}},\tag{2.10}$$

where γ is a parameter describing the inner slope, ρ_s is the scale density, and r_s is the scale radius, which we take to be $r_s = 21$ kpc.

3 Analytic Approximation

We will now consider an analytic approximation to J_S at small θ . For this purpose, we assume

- The J -factor at small θ is dominated by dark matter annihilation within the bulge, so we can ignore dark matter annihilation for $r > c_0$.
- The dark matter density within the bulge can be written as $\rho(r) \sim \rho_s(r/r_s)^{-\gamma}$. This is true for the generalized NFW profiles for which we obtained numerical results, but can encompass many more profiles.
- The gravitational potential within the bulge is dominated by Φ_{bary} , so we can ignore Φ_{DM} .
- Within the bulge, $\Phi_{bary}(r)$ is sufficiently well-approximated by a Taylor expansion to linear order in r .

Note, we will not always find these assumptions to be valid. As we will see in Section 3.1, some choices of the parameters will yield significant deviations from these assumptions, leading to deviations from the analytic prediction. We will address the import of deviations from the analytic treatment in Sections 3.1 and 4.

But given these assumptions, we find

$$\Phi(r) \sim \Phi_0 r, \quad (3.1)$$

where $\Phi_0 = G_N[(M_b/c_0^2) + M_d/2b_d^2]$, given our spherical approximation to the baryonic potential. But we will see that our result will apply for any value of Φ_0 . The only necessary condition is that the linear approximation to the potential be sufficiently good within the bulge.

We then find

$$\rho(r) = 4\sqrt{2}\pi (\Phi_0 r)^{3/2} \int_1^{\Phi(\infty)/\Phi_0 r} dx \sqrt{x-1} f(x\Phi_0 r). \quad (3.2)$$

For $r \ll c_0$, we may take $\Phi(\infty)/\Phi_0 r \rightarrow \infty$, in which case the only dependence of the integral on r is in the argument of f . Since $\rho(r) \propto r^{-\gamma}$, we can solve eq. 3.2 by assuming a power-law ansatz for f , namely

$$f(E) = f_0 E^{-\gamma-3/2},$$

$$f_0 = \rho_s(r_s \Phi_0)^\gamma \left[4\sqrt{2}\pi \int_1^\infty dx x^{-\gamma-3/2} \sqrt{x-1} \right]^{-1}. \quad (3.3)$$

Note that the integral in eq. 3.3 converges for $\gamma > 0$. In this case, the high-velocity tail of particles which can leave the bulge contribute negligibly to the density at small r .

We now have

$$P_n^2 = 8\pi^2 f_0^2 (\Phi_0 r)^{-2\gamma+(n/2)} \int_0^\infty dy_1 \int_0^\infty dy_2 y_1^2 y_2^2 \left((1/2)y_1^2 + 1 \right)^{-\gamma-3/2} \left((1/2)y_2^2 + 1 \right)^{-\gamma-3/2}$$

$$\times \frac{(y_1 + y_2)^{n+2} - |y_1 - y_2|^{n+2}}{(n+2)y_1 y_2 c^n},$$

$$= \left(f_0 \Phi_0^{-\gamma} \right)^2 (\Phi_0/c^2)^{(n/2)} I_{\gamma,n} r^{-2\gamma+(n/2)}, \quad (3.4)$$

where

$$I_{\gamma,n} \equiv 8\pi^2 \int_0^\infty dy_1 \int_0^\infty dy_2 y_1^2 y_2^2 \left(\frac{1}{2}y_1^2 + 1\right)^{-\gamma-3/2} \left(\frac{1}{2}y_2^2 + 1\right)^{-\gamma-3/2} \\ \times \frac{(y_1 + y_2)^{n+2} - |y_1 - y_2|^{n+2}}{(n+2)y_1 y_2}. \quad (3.5)$$

Note, however, that the integral defining $I_{\gamma,n}$ only converges for $\gamma > n/2$. For profiles which are not steep enough, the divergence at large velocity indicate that dark matter annihilation, even well within the bulge, is dominated by high-velocity particles which leave the bulge. Although such particles make only a negligible contribution to $\rho(r)$, the enhancement to the annihilation cross section for high-velocity particles when $n \geq 2\gamma$ means that they can dominate the annihilation rate.

If $\gamma > n/2$, however, we can find an analytic approximation to the J -factor of the GC within the inner few degrees. We will use our expression for $J_S(\cos\theta)$ (eq. 2.4), but only integrate to a distance c_0 from the GC, assuming that this region dominates the annihilation rate. This expression is thus restricted to the angular region $\theta \leq c_0/D \sim 4^\circ$, for which we can approximate $\sin\theta \sim \theta$. We then find

$$J_S(\cos\theta) = 2 \left(f_0^2 \Phi_0^{-2\gamma+(n/2)} c^{-n} \right) I_{\gamma,n} \int_{D\theta}^{c_0} dr \left(1 - \frac{D^2}{r^2} \theta^2 \right)^{-1/2} r^{-2\gamma+(n/2)}. \quad (3.6)$$

For $\theta \ll c_0/D$, we can take the upper limit of integration to infinity, in which case the integral has a power-law dependence on θ , yielding

$$J_S(\cos\theta) \sim 2D \left[(f_0/(\Phi_0 D)^\gamma)^2 (\Phi_0 D/c^2)^{n/2} I_{\gamma,n} \right] \left[\int_1^\infty dx (1-x^{-2})^{-1/2} x^{-2\gamma+(n/2)} \right] \\ \times \theta^{1-2\gamma+(n/2)}. \quad (3.7)$$

We thus see that, at small angles, there is a complete degeneracy between γ and n , provided the baryonic potential is dominant and $\gamma > n/2$. For a sufficiently steep profile satisfying this condition, the angular distribution of photon emission at small angles is independent of the dark matter distribution outside the bulge. This condition is satisfied for all reasonable models in the case of Sommerfeld-enhanced annihilation, and for even moderately cuspy profiles in the case of s -wave annihilation. But it is only satisfied for profiles cuspier than NFW in the case of p -wave annihilation, and for very steep profiles ($n > 2$) in the case of d -wave annihilation.

3.1 Validity of the Analytic Approximation

There are several considerations which affect whether or not this analytic approximation is valid. Provided the baryonic potential dominates over the dark matter gravitational potential, the velocity-distribution at the core (that is, at small E) is well-approximated by the analytic power-law form, as we illustrate in Figure 1. Here we plot $f(E)$ as a function of E , taking $\rho_s = 8 \times 10^6 M_\odot/\text{kpc}^3$, for various choices of γ (solid lines). We also plot the power-law analytic approximation (dashed lines). We see that, for profiles which are not too steep, the analytic approximation fits well at low energies. The analytic approximation begins to diverge from the numerical result for $\gamma \gtrsim 1.3$, when the dark matter contribution to the potential begins to dominate at small r . Note, however, that for smaller values of ρ_s ,

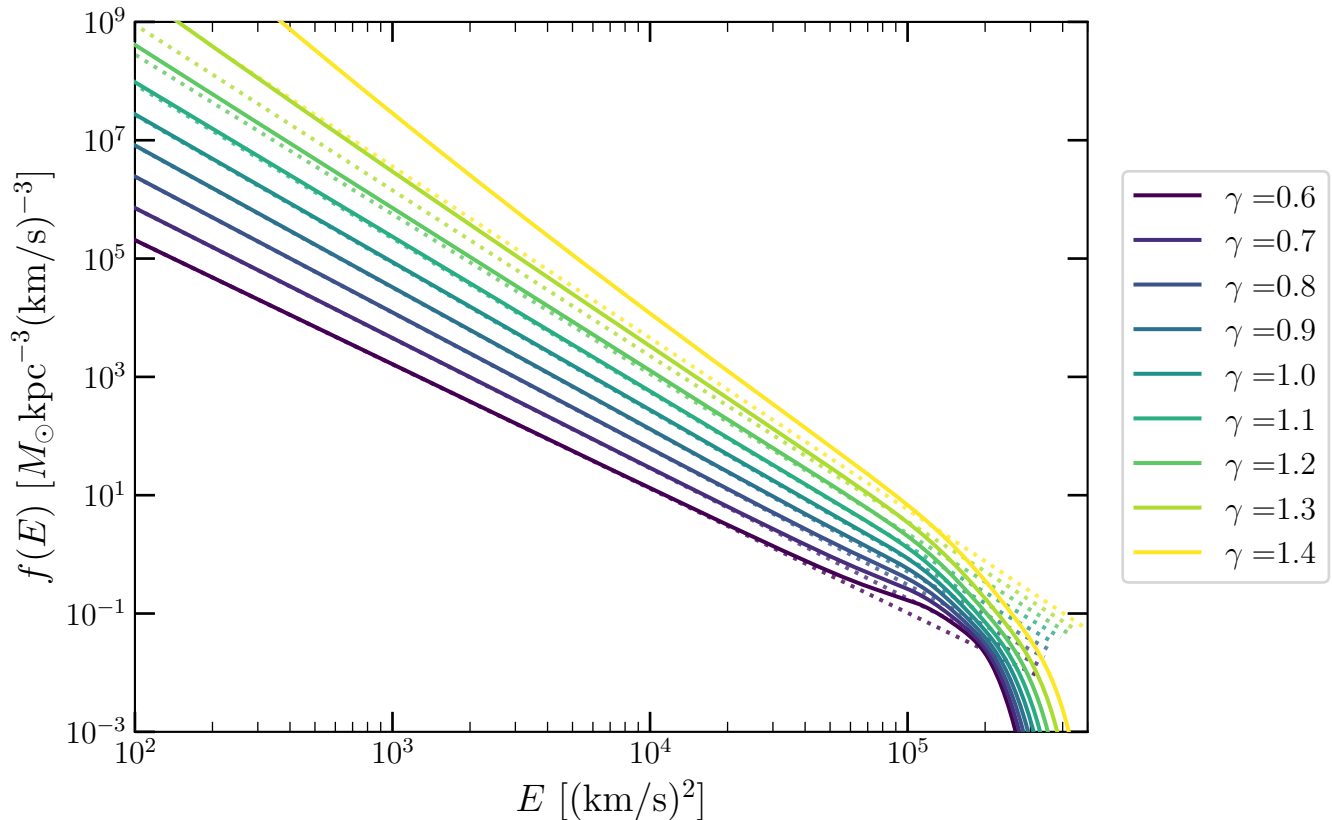


Figure 1: Plot of $f(E)$ as a function of E , assuming $\rho_s = 8 \times 10^6 M_\odot/\text{kpc}^3$, for various values of γ . The solid lines show the complete numerical calculation, while the dashed lines indicate the power-law analytic approximation.

the power-law result becomes a better approximation to the full numerical result, even for larger γ .

But even if the baryonic potential dominates, the linear approximation to this potential is only very good well within the bulge; at the edge of the bulge, the gravitational potential will necessarily deviate from the linear approximation, causing P_n^2 to deviate from power-law form at the edge of the bulge. This can cause the angular distribution to deviate from the analytic power-law form even at small angle, because the analytic approximation mismodels the velocity-distribution at the edge of the bulge, even along a line of sight aimed directly at the GC. The accuracy of the analytic approximation to the angular distribution thus depends on the steepness of the profile; for a steeper profile, with a larger fraction of the total annihilation rate concentrated deep in the interior of the bulge, the analytic result will be better. The larger the velocity power-law exponent n , the steeper the profile must be in order for the analytic approximation to be valid, since a larger value of n implies that dark matter annihilation is increasingly dominated by high-speed particles which explore the edges of the Bulge.

We thus see that changes to the steepness of the density slope within the bulge produce two competing effects. A steeper profile tends to concentrate dark matter annihilation deep within the bulge, making the analytic result a better approximation. More generally, for a

steeper profile, dark matter annihilation in the bulge is dominated by particles which never leave the bulge, implying that the angular distribution is determined only by the potential within the bulge, and is decoupled from what goes on outside. For a more shallow cusp, one must understand the details of how gravitational potential changes as one approaches the edge of the bulge. In this case, one would similarly expect that the effects of triaxiality, as well as deviations from the spherical approximation to the baryonic potential (due, for example to the Galactic disk contribution), will become more important. For larger n , one requires a steeper profile in order to decouple these effects, since the annihilation rate is increasingly dominated by high-speed particles which, though a small fraction of the dark matter within the bulge, nevertheless have an enhanced annihilation rate.

But the steeper the dark matter density slope, the more dark matter will tend to dominate the gravitational potential deep within the bulge, which would also invalidate the analytic approximation. The strength of the dark matter gravitational potential depends on both γ and ρ_s . If one assumes a generalized NFW profile throughout the entire MW halo, then one can estimate ρ_s , with uncertainties, from observational data throughout the halo. But if the dark matter distribution within the bulge forms a separate power-law distribution, then the normalization of the density distribution within the bulge is much less constrained, since it need only smoothly match onto a shallower generalized NFW outside the bulge.

As an illustrative example, we consider the case $\gamma = 1.2$, with $\rho_s = 4 \times 10^6 M_\odot/\text{kpc}^3$. For this choice, the dark matter density at the solar radius would be given by $\rho_\odot = 0.25 \text{ GeV}/\text{cm}^3$. In Figure 2, top panel, we plot the potential $\Phi(r)$, including the baryonic and dark matter contributions, as well as the total potential. The solid lines are the full potential, while the dashed lines represent the analytic power-law approximation which we consider. We see that, for this choice of γ and ρ_s , the baryonic contribution dominates the total potential, which is required for the analytic approximation to be valid. But the power-law approximation to the baryonic potential breaks down once we reach the edge of the bulge, for $r \gtrsim \mathcal{O}(0.1) \text{ kpc}$. As such, we expect deviations from the analytic approximation to be driven by particles which explore the edge of the bulge.

In the middle panel of Figure 2, we plot P_n^2 for $n = -1, 0, 2$ and 4. Again, the complete numerical calculation is shown in solid lines, while the power law analytic approximation is shown in dashed lines. For $n = 0$, the ordinary case of s -wave annihilation, the analytic approximation is nearly exact within the bulge, since dark matter annihilation is velocity-independent, so deviations from the analytic approximation to the potential are irrelevant. For the case of Sommerfeld-enhanced annihilation ($n = -1$), the analytic approximation to $P_{n=-1}^2$ matches the numerical calculation well inside the bulge, because for Sommerfeld-enhanced annihilation, the annihilation rate is dominated by low-speed particles which never explore the edges of the bulge, where the potential deviates from power-law. For p -wave annihilation ($n = 2$), we see that the power law approximation is only a good fit deep within the bulge. This is not surprising, since the profile we have chosen is only slightly steeper than the limit $\gamma = 1$, at which the analytic approximation breaks down entirely for p -wave annihilation, which is then dominated by particles which leave the bulge.

In the bottom panel of Figure 2, we plot the angular distribution, which is proportional to $J_S(\cos\theta)$, for $n = -1, 0, 2$ and 4. The angular distribution is normalized to unity when integrated over 4° , and is plotted with solid lines. We used dashed lines to plot the power-law analytic approximation to $J_S(\cos\theta)$, which is normalized (for ease in comparing to the numerical result) to match the numerical computation as $\theta \rightarrow 0$. As expected from the

discussion of P_n^2 , the slope of analytic approximation matches the that of the numerical computation fairly well within the inner degree, for Sommerfeld-enhanced annihilation. On the other hand, for the case of p -wave annihilation, the angular distribution matches the analytic prediction only for a very small angular range ($\Delta\theta \sim \mathcal{O}(10^{-3})$ degrees), which would not be useful for a data analysis.

It is interesting to note that, for this case ($\gamma = 1.2$), the photon angular distribution arising from Sommerfeld-enhanced annihilation is a well-matched by the analytic approximation to the GC because dark matter annihilation is dominated by low-speed particles which only explore the bulge. This result thus largely depends only on the slope of the dark matter distribution within the bulge, and is independent of the dark matter distribution outside the bulge. This analytic approximation can thus be generalized beyond the assumption of an NFW profile, and does not assume that the slope of the profile inside the bulge is that same as that outside. Similarly, it is relatively robust against the effects of triaxiality, which is likely to affect the dark matter profile at relatively large distances from the GC.

On the other hand, the analytic approximation to p -wave fails (except at very small angles) because dark matter annihilation is, in this case, dominated by high-speed particles which can leave the bulge. Interestingly, this is the case even though, for $\gamma = 1.2$, the analytic approximation to the velocity distribution matched the numerical calculation fairly well (see Figure 1). Beyond the failure of the analytic approximation to the angular distribution, the more general lesson is that, for p -wave annihilation in the case of a profile which is not very steep, the angular distribution near the GC cannot be determined accurately without a full knowledge of the dark matter profile and baryonic potential, even far away from the GC. Similarly, the effects of triaxiality, which are expected to be relatively small within the Galactic bulge, should be expected to nevertheless have a significant effect on the angular distribution at small angles. Even though a negligible fraction of the DM within the Galactic bulge may explore the gravitational potential very far away, that small fraction of particles will dominate the annihilation rate (and thus the angular distribution) unless the profile is very steep. The considerations are even more relevant for the case of d -wave annihilation.

4 The Galactic Center Excess

As an application, we consider the GC excess. The excess arises in photons with an energy of a few GeV, at which the Fermi-LAT would have an angular resolution of order a few tenths of a degree. But for the purpose of understanding how well the analytic approximation works, and when and why it fails, we will consider angles as small as 10^{-3} degrees from the GC.

For the case of s -wave dark matter annihilation ($n = 0$), the angular distribution of the GC excess would require an inner slope within the bulge of $\gamma = 1.2 - 1.4$ [2, 23]. For p -wave annihilation ($n = 2$), the same morphology would require $\gamma = 1.7 - 1.9$, if the analytic approximation is valid. This range of γ is steep enough that dark matter annihilation deep within the bulge would be dominated by particles which never left the bulge. Note that, although this is a much steeper profile than is usually considered, the slope may be much shallower outside the bulge. A model of d -wave annihilation would also match the angular distribution of the GC excess if $\gamma = 2.2 - 2.4$. We will focus on the case of p -wave annihilation, with $\gamma = 1.7$.

But for such a steep profile the baryonic contribution to the gravitational potential may no be longer dominant. This may be the case, but need not be. One can always reduce the amplitude of the dark matter density within the bulge, in order to ensure that the bary-

onic potential dominates, with the amplitude of the GC excess obtained by a corresponding rescaling of $(\sigma v)_0$. However, if the dark matter density at the edge of the bulge is too small, it would be difficult to obtain a density at the solar radius which is consistent with observational data. If the dark matter density at the solar radius is $0.3 \text{ GeV}/\text{cm}^3$, and if the profile outside the bulge is NFW with $r_s = 21 \text{ kpc}$, then the dark matter density at $r = c_0$ would be $\rho_{c_0} = 2 \times 10^8 M_\odot/\text{kpc}^3$. Setting $\rho_{c_0} = \rho_s (c_0/r_s)^{-1.7}$, we would find $\rho_s = 5 \times 10^5 M_\odot/\text{kpc}^3$. If we had instead assumed that the dark matter density between the edge of the bulge and scale radius had a slope of only -0.6 , this would have reduced ρ_{c_0} , and in turn ρ_s , by a factor of 2.5. We will consider the cases $\rho_s = 4 \times 10^a M_\odot/\text{kpc}^3$, with $a = 3, 4, 5, 6$.

In determining the angular distribution with a full numerical calculation, it is necessary to make some assumption for the profile outside the bulge. For simplicity, we will assume a generalized NFW profile with inner slope of $\gamma = 1.7$ throughout the MW halo. But as we have noted, such a steep profile may not be valid outside the bulge. To characterize the extent to which DM annihilation outside the bulge affects the angular distribution, we will perform the numerical calculation in two ways. First, we compute the complete angular distribution assuming a generalized NFW profile. Second, we will compute the velocity-distribution assuming a generalized NFW profile throughout the MW halo, but will compute the J -factor by assuming that there is no dark matter annihilation outside the Bulge. This amounts to taking the upper limit of integration in eq. 2.4 to be c_0 .

We plot our results in Figure 3. The solid lines indicate the numerically-computed angular distribution for the case of p -wave annihilation, normalized so that the integral to 4° is unity. The dashed lines are similar, but neglecting dark matter annihilation outside of the core. Finally, the dotted line is the analytic approximation, which is normalized to match the numerical calculation for $\rho_s = 4 \times 10^3 M_\odot/\text{kpc}^3$ as $\theta \rightarrow 0$. Note that the solid and dashed lines are nearly identical. This implies that, at small angles, the dark matter annihilation rate is indeed dominated by particles which annihilate within the bulge itself.

We see that, as ρ_s decreases, the analytic approximation becomes a better match to the numerical calculation, for a larger range of angles. This is to be expected, because, this limit amounts to a best case scenario, where the profile is steep enough that even the high-speed particles which dominate p -wave annihilation are less likely to explore the edge of the bulge. But the dark matter density within the bulge is also taken to be small enough that the dark matter does not deform the potential significantly. But even in this case, we see that the analytic approximation begins to diverge from the numerical calculation for angles of $\mathcal{O}(0.1^\circ)$. This essentially happens because, no matter how steep the profile, the effect can only be to concentrate particles near the GC. To the extent that the baryonic potential dominates the profile, there will always be a very small high-speed tail of particles which can reach the edge of the bulge, but this small tail will nevertheless give a large contribution to the annihilation rate for the case of p -wave annihilation.

We may thus draw a broader lesson from the comparison of the analytic approximation to the numerical calculation of the angular distribution in the limit of small ρ_s . The difference between these curves roughly characterizes the dependence of the angular distribution, even well within the bulge, on particles which leave the bulge, and thus the level of uncertainty in the angular distribution introduced by variations in the dark matter profile form, triaxiality, or any other features of the dark matter or baryonic distribution outside the bulge.

It is also interesting to note that, as ρ_s increases, the steepness of the angular distribution at small angles also increases. This result can also be understood intuitively. As ρ_s increases, the dark matter contribution to the gravitational potential becomes more important. In the

limit in which the dark matter contribution to the potential dominates, we may ignore the baryons entirely. This problem was considered in [32], where it was found that the angular distribution (at small angle) for p -wave annihilation is a power law with slope $3 - 3\gamma$. We would thus expect the slope of the angular distribution to increase by a factor of $3/2$, as ρ_s increases. This result is confirmed in Figure 3, where the choice $\rho_s = 4 \times 10^6 M_\odot/\text{kpc}^3$ leads to an angular distribution with a slope of ~ -2.1 at small angle.

Interestingly, if the angular distribution is to have slope -1.4 at small angle (as one would expect for s -wave annihilation with $\gamma = 1.2$), then for p -wave annihilation in a dark matter-dominated halo, one would require $\gamma \sim 1.47$. Out to distances of a few kpc, for which the small angle approximation is still valid, the gravitational potential varies between being either baryon-dominated or dark matter-dominated. If p -wave annihilation were to produce an angular distribution consistent with what is observed for the GC excess, one would expect the slope of the dark matter density profile to lie in the $\gamma \sim 1.5 - 1.7$ range.

Note that, in the case of p - or d -wave annihilation, a steeper slope within the inner slope region could also lead to a larger rate for dark matter annihilation near the black hole at the center of the MW [31, 33]. We have not included the effects of this on our analysis, but this would be an interesting topic for future work.

5 Conclusion

We have considered velocity-dependent dark matter annihilation within the Galactic bulge. Because the rate of velocity-dependent annihilation at any given location depends not only on the dark matter density at that point, but on the gravitational potential at all locations sampled by particles passing through that point, determining the annihilation rate can be a very non-local problem. Our goal has been to understand the extent to which the angular distribution of photons arriving from the direction of the bulge can be understood entirely using features of the dark matter and baryonic density distributions within the bulge. Because the behavior of the gravitational potential within the bulge is very different from its behavior far away, the behavior of the dark matter density profile may also be quite different from what is expected from simulations which are extrapolated to small distances. There are large uncertainties in our ability to probe the dark matter profile in baryon-rich environments such as the bulge, either using simulations or stellar tracers, making it important to understand how strongly these environments control the angular distribution.

The GeV excess of photons from the GC may have its origin in dark matter annihilation. But such solutions are constrained by searches for photons from other dark matter-rich environments, such as dSphs. Scenarios of velocity-dependent dark matter annihilation can avoid such constraints, which makes it particularly interesting to determine not only if these scenarios can reproduce the observed angular distribution, but also to determine which features of distribution contribute to this determination.

We have found that for the case of Sommerfeld-enhanced annihilation, dark matter annihilation within the bulge is typically dominated by slow-moving particles which never leave the bulge. In this case, the photon angular distribution at small angle is largely controlled by a single parameter: the dark matter density slope within the bulge. The behavior of the dark matter distribution outside the bulge, including the slope in the region between the bulge and the scale radius, has only a small effect. In this case, the photon angular distribution largely probes the localized astrophysics of dark matter within the bulge, which can be robustly

reconstructed if the angular resolution (for the energy range of the photons produced by DM annihilation) is $\lesssim 0.1^\circ$.

On the other hand, for p - or d -wave annihilation, dark matter annihilation within the bulge receives a significant contribution from high-speed particles which leave the bulge. Although this is a small fraction of the dark matter particles within the bulge, this energetic tail nevertheless dominates the annihilation rate for these particular scenarios of velocity-dependent annihilation. In this case, the photon angular distribution, even at small angle, necessarily depends on the dark matter profile and the gravitational potential well outside the bulge. As a result, uncertainties in the dark matter profile, including the effects of triaxiality and the way the dark matter density interpolates between its behavior within and outside the bulge, will necessarily have a non-trivial impact on the angular distribution.

The GC excess, as currently understood, would be consistent with s -wave dark matter annihilation with a density slope of $\gamma = 1.2 - 1.4$. To alleviate constraints from dSphs searches, one would like to consider a scenario of p -wave annihilation. Our results have shown that, in this case, it is not possible to cleanly relate this angular distribution to the slope of the density profile. Instead, we find a general prediction that this angular distribution would require a steeper profile in the case of p -wave annihilation. For example, the angular distribution (at small angle) yielded by s -wave annihilation with $\gamma = 1.2$ inside the bulge, would be yielded with p -wave annihilation with $\gamma \sim 1.5 - 1.7$, with the details determined by parameters such as the ratio of baryons to dark matter in the MW, the slope of the dark matter distribution outside the bulge, triaxiality, etc.

Note, we have not attempted an actual fit to data from the GC. Instead, we have simply taken at face value the detailed analyses performed in previous works, which have considered Fermi data from the GC as well as a variety of backgrounds in order to assess the morphology of the excess. But millisecond pulsars may generate part or all of the GC excess. Even assuming a large contribution to the excess arises from DM annihilation, correct inclusion of a MSP contribution could change the morphology of the contribution arising from DM annihilation. Similarly, improvements in our understanding of other backgrounds could also modify our understanding of the excess morphology. Although this would modify the details of our analysis, the overall framework would remain unchanged. A more detailed study of p -wave annihilation as an explanation for the GC excess seen in Fermi data would be an interesting topic of future work.

Acknowledgements

We are grateful to Pearl Sandick and Louis E. Strigari for useful discussions. JK is supported in part by DOE grant DE-SC0010504. JR is supported by NSF grant AST-1934744.

References

- [1] Lisa Goodenough and Dan Hooper. Possible Evidence For Dark Matter Annihilation In The Inner Milky Way From The Fermi Gamma Ray Space Telescope. 10 2009.
- [2] Dan Hooper and Lisa Goodenough. Dark Matter Annihilation in The Galactic Center As Seen by the Fermi Gamma Ray Space Telescope. *Phys. Lett. B*, 697:412–428, 2011. doi: 10.1016/j.physletb.2011.02.029.
- [3] M. Ajello et al. Fermi-LAT Observations of High-Energy γ -Ray Emission Toward the Galactic Center. *Astrophys. J.*, 819(1):44, 2016. doi: 10.3847/0004-637X/819/1/44.

- [4] Kevork N. Abazajian. The Consistency of Fermi-LAT Observations of the Galactic Center with a Millisecond Pulsar Population in the Central Stellar Cluster. *JCAP*, 03:010, 2011. doi: 10.1088/1475-7516/2011/03/010.
- [5] A. A. Abdo et al. Observations of Milky Way Dwarf Spheroidal galaxies with the Fermi-LAT detector and constraints on Dark Matter models. *Astrophys. J.*, 712:147–158, 2010. doi: 10.1088/0004-637X/712/1/147.
- [6] M. Ackermann et al. Constraining Dark Matter Models from a Combined Analysis of Milky Way Satellites with the Fermi Large Area Telescope. *Phys. Rev. Lett.*, 107:241302, 2011. doi: 10.1103/PhysRevLett.107.241302.
- [7] M. Ackermann et al. Dark Matter Constraints from Observations of 25 Milky Way Satellite Galaxies with the Fermi Large Area Telescope. *Phys. Rev. D*, 89:042001, 2014. doi: 10.1103/PhysRevD.89.042001.
- [8] M. Ackermann et al. Searching for Dark Matter Annihilation from Milky Way Dwarf Spheroidal Galaxies with Six Years of Fermi Large Area Telescope Data. *Phys. Rev. Lett.*, 115(23):231301, 2015. doi: 10.1103/PhysRevLett.115.231301.
- [9] A. Albert et al. Searching for Dark Matter Annihilation in Recently Discovered Milky Way Satellites with Fermi-LAT. *Astrophys. J.*, 834(2):110, 2017. doi: 10.3847/1538-4357/834/2/110.
- [10] Laura J. Chang, Mariangela Lisanti, and Siddharth Mishra-Sharma. Search for dark matter annihilation in the Milky Way halo. *Phys. Rev. D*, 98(12):123004, 2018. doi: 10.1103/PhysRevD.98.123004.
- [11] Dan Hooper, Rebecca K. Leane, Yu-Dai Tsai, Shalma Wegsman, and Samuel J. Witte. A systematic study of hidden sector dark matter: application to the gamma-ray and antiproton excesses. *JHEP*, 07(07):163, 2020. doi: 10.1007/JHEP07(2020)163.
- [12] Brant E. Robertson and Andrew R. Zentner. Dark matter annihilation rates with velocity-dependent annihilation cross sections. *Physical Review D*, 79(8), apr 2009. doi: 10.1103/physrevd.79.083525. URL <https://doi.org/10.1103/PhysRevD.79.083525>.
- [13] Francesc Ferrer and Daniel R. Hunter. The impact of the phase-space density on the indirect detection of dark matter. *JCAP*, 09:005, 2013. doi: 10.1088/1475-7516/2013/09/005.
- [14] Kimberly K. Boddy, Jason Kumar, Louis E. Strigari, and Mei-Yu Wang. Sommerfeld-Enhanced J -Factors For Dwarf Spheroidal Galaxies. *Phys. Rev. D*, 95(12):123008, 2017. doi: 10.1103/PhysRevD.95.123008.
- [15] Yi Zhao, Xiao-Jun Bi, Peng-Fei Yin, and Xinmin Zhang. Constraint on the velocity dependent dark matter annihilation cross section from gamma-ray and kinematic observations of ultrafaint dwarf galaxies. *Phys. Rev. D*, 97(6):063013, 2018. doi: 10.1103/PhysRevD.97.063013.
- [16] Mihael Petac, Piero Ullio, and Mauro Valli. On velocity-dependent dark matter annihilations in dwarf satellites. *JCAP*, 12:039, 2018. doi: 10.1088/1475-7516/2018/12/039.
- [17] Thomas Lacroix, Martin Stref, and Julien Lavalle. Anatomy of Eddington-like inversion methods in the context of dark matter searches. *JCAP*, 09:040, 2018. doi: 10.1088/1475-7516/2018/09/040.
- [18] Kimberly K. Boddy, Jason Kumar, Jack Runburg, and Louis E. Strigari. Angular distribution of gamma-ray emission from velocity-dependent dark matter annihilation in subhalos. *Phys. Rev. D*, 100(6):063019, 2019. doi: 10.1103/PhysRevD.100.063019.
- [19] Kimberly K. Boddy, Jason Kumar, and Louis E. Strigari. Effective J -factor of the Galactic Center for velocity-dependent dark matter annihilation. *Phys. Rev. D*, 98(6):063012, 2018. doi: 10.1103/PhysRevD.98.063012.

- [20] Christian Johnson, Regina Caputo, Chris Karwin, Simona Murgia, Steve Ritz, and Jessie Shelton. Search for gamma-ray emission from p -wave dark matter annihilation in the Galactic Center. *Phys. Rev. D*, 99(10):103007, 2019. doi: 10.1103/PhysRevD.99.103007.
- [21] Erin Board, Nassim Bozorgnia, Louis E. Strigari, Robert J. J. Grand, Azadeh Fattahi, Carlos S. Frenk, Federico Marinacci, Julio F. Navarro, and Kyle A. Oman. Velocity-dependent J-factors for annihilation radiation from cosmological simulations. *JCAP*, 04:070, 2021. doi: 10.1088/1475-7516/2021/04/070.
- [22] Daniel McKeown, James S. Bullock, Francisco J. Mercado, Zachary Hafen, Michael Boylan-Kolchin, Andrew Wetzel, Lina Necib, Philip F. Hopkins, and Sijie Yu. Amplified J-factors in the Galactic Centre for velocity-dependent dark matter annihilation in FIRE simulations. *Mon. Not. Roy. Astron. Soc.*, 513(1):55–70, 2022. doi: 10.1093/mnras/stac966.
- [23] Francesca Calore, Ilias Cholis, and Christoph Weniger. Background Model Systematics for the Fermi GeV Excess. *JCAP*, 03:038, 2015. doi: 10.1088/1475-7516/2015/03/038.
- [24] Jason Kumar and Danny Marfatia. Matrix element analyses of dark matter scattering and annihilation. *Phys. Rev. D*, 88(1):014035, 2013. doi: 10.1103/PhysRevD.88.014035.
- [25] Federica Giacchino, Laura Lopez-Honorez, and Michel H. G. Tytgat. Scalar Dark Matter Models with Significant Internal Bremsstrahlung. *JCAP*, 10:025, 2013. doi: 10.1088/1475-7516/2013/10/025.
- [26] Takashi Toma. Internal Bremsstrahlung Signature of Real Scalar Dark Matter and Consistency with Thermal Relic Density. *Phys. Rev. Lett.*, 111:091301, 2013. doi: 10.1103/PhysRevLett.111.091301.
- [27] Nima Arkani-Hamed, Douglas P. Finkbeiner, Tracy R. Slatyer, and Neal Weiner. A Theory of Dark Matter. *Phys. Rev. D*, 79:015014, 2009. doi: 10.1103/PhysRevD.79.015014.
- [28] Jonathan L. Feng, Manoj Kaplinghat, and Hai-Bo Yu. Sommerfeld Enhancements for Thermal Relic Dark Matter. *Phys. Rev. D*, 82:083525, 2010. doi: 10.1103/PhysRevD.82.083525.
- [29] Louis E. Strigari and Roberto Trotta. Reconstructing WIMP Properties in Direct Detection Experiments Including Galactic Dark Matter Distribution Uncertainties. *JCAP*, 11:019, 2009. doi: 10.1088/1475-7516/2009/11/019.
- [30] Miguel Pato, Louis E. Strigari, Roberto Trotta, and Gianfranco Bertone. Taming astrophysical bias in direct dark matter searches. *JCAP*, 02:041, 2013. doi: 10.1088/1475-7516/2013/02/041.
- [31] Pearl Sandick, Kuver Sinha, and Takahiro Yamamoto. Black Holes, Dark Matter Spikes, and Constraints on Simplified Models with t -Channel Mediators. *Phys. Rev. D*, 98(3):035004, 2018. doi: 10.1103/PhysRevD.98.035004.
- [32] Bradley Boucher, Jason Kumar, Van B. Le, and Jack Runburg. J-factors for velocity-dependent dark matter annihilation. *Phys. Rev. D*, 106(2):023025, 2022. doi: 10.1103/PhysRevD.106.023025.
- [33] Jessie Shelton, Stuart L. Shapiro, and Brian D. Fields. Black hole window into p -wave dark matter annihilation. *Phys. Rev. Lett.*, 115(23):231302, 2015. doi: 10.1103/PhysRevLett.115.231302.

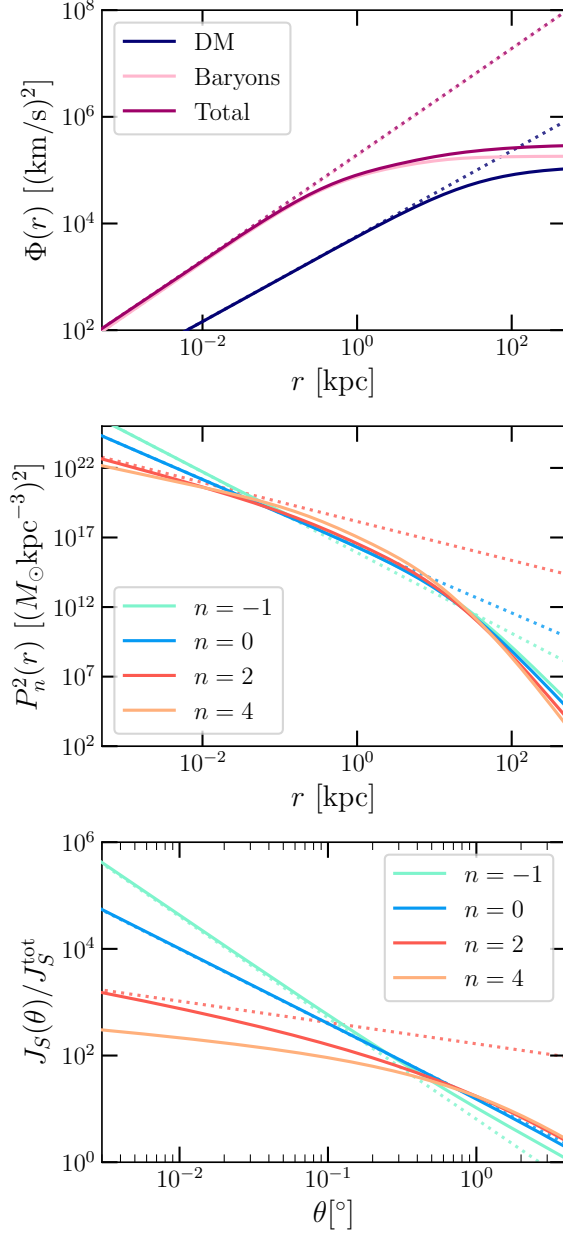


Figure 2: The top panel shows the gravitational potential Φ for the DM contribution, baryonic contribution, and the total potential for an NFW distribution with $\gamma = 1.2$ and $\rho_s = 4 \times 10^6 M_\odot/\text{kpc}^3$. In all three panels, the dotted lines show the analytic approximation for comparison. The middle panel shows $P_n^2(r)$ for all n considered. The bottom panel shows the J -factor distributions $J_S(\theta)$ for all n considered normalized by $J_S^{\text{tot}} \equiv \int_0^{4\pi/180} d\theta \sin\theta J_S(\cos\theta)$. The analytic comparisons for the normalized J -factors are matched to the numerical calculations at $\theta = 1 \times 10^{-3}$ degrees for ease of comparison.

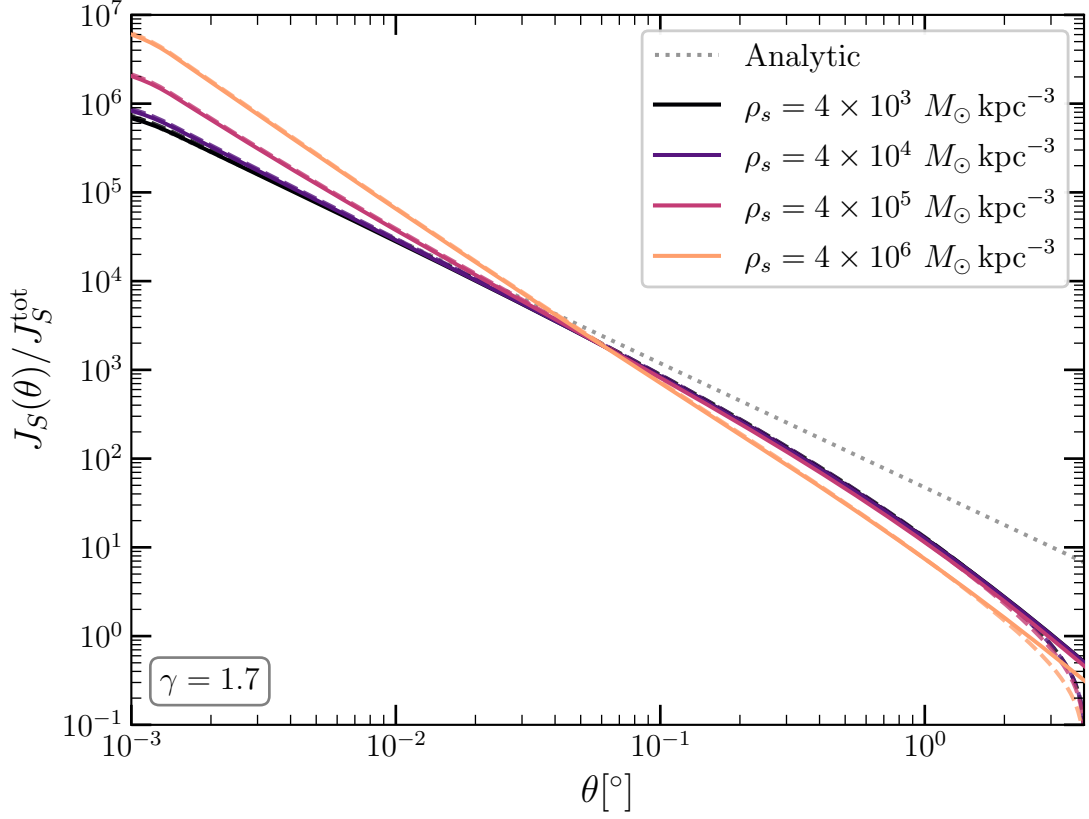


Figure 3: J -factors for varying ρ_s values for an NFW distribution with $\gamma = 1.7$ normalized by $J_S^{\text{tot}} \equiv \int_0^{4\pi/180} d\theta \sin\theta J_S(\cos\theta)$. The numerical calculations with the DM annihilation truncated outside the bulge are shown as dashed lines. The analytic approximations are matched to the numerical calculations at $\theta = 1 \times 10^{-3}$ degrees for ease of comparison.